ACS Catalysis

Research Article

pubs.acs.org/acscatalysis

Enzymatic Flexibility and Reaction Rate: A QM/MM Study of HIV-1 Protease

António J. M. Ribeiro,[†,‡] Diogo Santos-Martins,[†] Nino Russo,[‡] Maria J. Ramos,[†] and Pedro A. Fernandes*[,†]

[†]UCBIO, REQUIMTE, Departamento de Química e Bioquímica, Faculdade de Ciências da Universidade do Porto, Rua do Campo Alegre, 4169-007 Porto, Portugal

[‡]Dipartimento di Chimica, Università della Calabria, 87036 Arcavacata di Rende, Italia

Supporting Information

ABSTRACT: The relevance of conformational fluctuations on enzyme rates has been a matter of debate for decades. Single molecule experiments have detected variations on the catalytic rates between different enzyme molecules, and within the same enzyme molecule, in a time scale larger than turnover. Computational methods can detect different energy barriers, induced by thermal conformational fluctuations, at a microscopic time scale, several orders of magnitude faster than the turnover rate of the fastest enzyme. Others have observed these barrier fluctuations, but few computational studies have dissected them in detail and tried to understand their origins and consequences. For this purpose, we studied the first step of the reaction catalyzed by HIV-1 Protease, starting from 40 different conformations. We found activation free energies ranging from 14.5 to 51.3 kcal·mol^{-1}. The calculated apparent barrier is 16.5 kcal·mol^{-1}, which is very close to the experimental value of 15.9 kcal·mol^{-1} for product release. These fluctuations are determinant to the overall rate, and these are correlated to specific structural changes. The effect of each enzymatic conformation on the stabilization of the transition state can be explained by the electrostatic interaction of every protein residue with the flow of net electronic density (negative charge) from the reactants to the transition state.

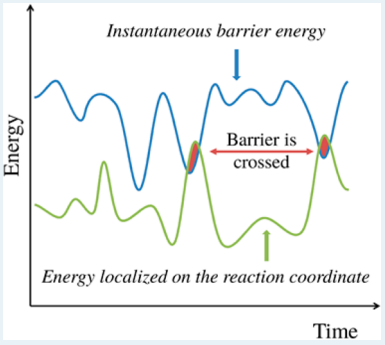

KEYWORDS: *enzymatic catalysis, QM/MM, instantaneous disorder, transition-state theory, protein dynamics*

1. INTRODUCTION

Enzyme structures fluctuate over time on a multidimensional free-energy landscape.[1−4] Even at equilibrium, a broad enzymatic state such as the "enzyme−substrate complex" is a blend of innumerable interchanging conformations. This complexity extends to catalysis: there are countless possible transition-state geometries connecting reactant conformations to product conformations. Conventional experimental kinetic studies overlook this diversity, because they measure properties of ensembles of enzymes, which are averaged over time and over moles of molecules. Enzymatic rates from single molecule experiments, however, present both what has been coined as *static disorder* (rate differences on different enzymatic molecules, assumed to be due to rate variations much slower than turnover) and *dynamic disorder* (rate differences on the same enzymatic molecule along a time close to turnover).[5] Initially, it was thought that folding fluctuations slower than the time of the experiment caused *static disorder*,[6,7] while faster structural fluctuations caused dynamic disorder.[6,8] It is now accepted that intrinsic structural differences, such as the existence of post-translational modifications, or of truncated or partially folded enzymes,[9,10] account for most cases of *static disorder*. As for *dynamic disorder*, it was shown that it is not a universal characteristic, as there are proteins that do not display it.[10−12]

Theoretical modeling of enzymes has been vital to the progress of the field of enzymatic catalysis. Most notably, computational methods are the only systematic approach to describe the reaction pathways followed by enzymes at an atomic level:[13−17] Enzymatic reactions can be modeled today for the whole enzyme with quantum mechanics/molecular mechanics (QM/MM) methods and chemical accuracy. There is a growing number of theoretical studies that focus on the link between structural flexibility and its effect on enzymatic catalysis. One of the main observations is that the calculated activation energies are dependent on the chosen initial structure for the reactants.[18−26] Depending on the exact methodology or enzyme, differences on the barrier between 5 kcal·mol^{-1}[23,26] and more than 30 kcal·mol^{-1}[18,21] have been found. Some explanations for the relation between the differences in the structure and in the barriers have been proposed,[18,23,26] but they are mostly structural considerations, like specific distances between active center atoms, and hence

Received: April 11, 2015
Revised: August 3, 2015
Published: August 20, 2015

DOI: 10.1021/acscatal.5b00759
ACS Catal. 2015, 5, 5617−5626

specific to the enzymes in question. In this paper, we explored in greater detail the electrostatic interactions of noncatalytic residues with the active center, and found that, in conjunction with different active site conformations, they are the main cause for instantaneous barrier fluctuations. In principle, this kind of analysis can be applied to any enzyme.

For the sake of clarity, we introduce the concept of *instantaneous disorder*. It is impossible to reconcile the dispersion in the barriers obtained by computational methods with the dispersion obtained from experimental data on *dynamic disorder* due to the altogether different time scales considered. *Dynamic disorder* reflects variability in conformations that occur in a time scale larger than k_{cat}. Computational methods, on the other side, have only access to much smaller time scales. *Instantaneous disorder* is then the instantaneous fluctuations in the enzyme structure with a time scale much smaller than k_{cat}, which leads to different activation barriers. We picture a free-energy profile for the reaction that is constantly changing, with innumerable different possible energy barriers that change both quantitatively (different energies) and qualitatively (different paths). The barriers affected by *instantaneous disorder* cannot be measured experimentally because most of them are never crossed. Figure 1 is illustrative

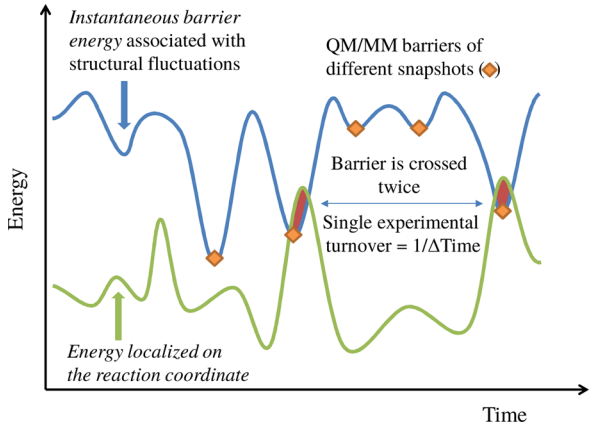

Figure 1. Model for the catalytic landscape of enzymes and its relation with QM/MM results.

of this model. We consider two independent motions: the movement of all the residues in the enzyme, which leads to different energy barriers; and the movement of the atoms in the reaction coordinate. The reaction can only take place when the energy localized on the reaction coordinate (bottom line) is enough to overcome the barrier provided by the enzymatic conformation at that time (top line). The effect of the enzyme scaffold in the barrier is given by its instantaneous interactions (mostly electrostatic) with the active center. Variations in the enzyme structure affect the barrier only through changes in these instantaneous interactions. It is obvious that these two motions are not truly independent, but for the sake of the argument, it is only necessary that the existent correlation is not the cause of the observed rate.

In this work, we used 40 conformations taken from a molecular dynamics (MD) simulation of HIV-1 protease to obtain 40 free energy profiles of its catalytic mechanism with a QM/MM methodology. HIV-1 protease was chosen as model enzyme due to its small size and simplicity: Protease consists of two identical chains of 99 residues,[27,28] and it has only two (aspartic) catalytic residues.[27−35] Furthermore, its mechanism is well established from experimental[29−37] and theoretical[38−40] standpoints, as well as from studies on other aspartic proteases.[41−45] To limit the MD sampling to productive conformations, we fixed a hydrogen bond between the protonated oxygen of Asp25B and the carbonyl oxygen of the scissile peptide bond. This hydrogen bond is also found in an ensemble of unconstrained structures, but its occupancy is quite low. The entropic cost of such constraint was calculated recently to be 4.6 kcal·mol^{-1} at physiological temperature.[46] This contribution was added to all the barriers in order to compare them directly with the experimental turnover, which constitutes an upper limit for the chemical step, as product release is rate limiting.

The active center of each structure was inspected to identify geometric parameters important to the barrier. Furthermore, to understand the effect of every protease residue in catalysis, we employed a method where each residue was removed from both reactant and transition state structures. By comparing the barriers in the "deleted" systems with the barriers in the complete enzyme, we were able to define exactly the contribution of the 198 residues to catalysis in each of the 40 models.

We observed a highly heterogeneous catalysis landscape with activation energies ranging from 14.5 to 51.3 kcal·mol^{-1}. We found that different reaction paths and different conformations in the active center led to different barriers, as expected. However, even initial structures that led to the same mechanism and had very similar active center geometries presented large barrier heterogeneity. The main cause behind the dispersion in these barriers are oscillations of the electrostatic interactions (coming from Coulomb and van der Waals forces) between the active center and the rest of the enzyme due to thermal conformational fluctuations. Our results show consistently that residues that help the flow of negative charge toward the scissile peptide bond will decrease the barrier, while residues that hinder such flow of negative charge density increase the barrier. An analysis of the different positioning of these residues in the conformations is enough to explain why barriers oscillate so much. Further studies will be necessary to assess if this conclusion can be generalized to more enzymes. It is tempting to hypothesize that the effect will be important in enzymes where the charge distribution is very different in the reactants and transition-state structure, whereas it will be less important in free-radical reactions, for example.

2. METHODS

The overall computational protocol in this work followed these steps: (a) Modeling of the enzyme−substrate complex from the 4HPV PDB structure; (b) Molecular dynamics simulations (10 + 5 ns) to stabilize the modeled structure; (c) Three independent MD simulations (total of 80 ns) to sample the conformational space of the system; (d) QM/MM calculation of the reactants and transition state of the first step of the reaction for 40 different initial structures, resulting from the previous molecular dynamics simulations, by unconstrained geometry optimization of both stationary points at the ONIOM(B3LYP/6-311+g(2d,2p)|AMBER) level; (e) Assessment of the influence of every residue in the activation energy for each one of the 40 structures.

The protease model was built from the X-ray structure 4HPV.[47] This structure contains the entire HIV-1 protease bond to the substrate-based inhibitor Ac-Thr-Ile-Nle-[CH_2−NH]-Nle-GIn-Arg.amide. We modeled the inhibitor into the

DOI: 10.1021/acscatal.5b00759
ACS Catal. 2015, 5, 5617−5626

Ac-Thr-Ile-Met-[CO-NH]-Met-GIn-Arg.amide substrate by changing the [CH2-NH] group to an amide [CO-NH] group, and the Nle (Norleucine) residues to methionine residues. In addition, we added the catalytic water into the active center, and protonated Asp25B. This residue is experimentally known to be protonated to fulfill its role in the catalytic mechanism. This model contains 3232 atoms. The modeling task was done in the GaussView software.[48]

In order to equilibrate the modeled structure, we did a 10 ns molecular dynamics simulation without any structural restrictions. During this simulation, the active center adopted a conformation that was not adequate to the catalytic reaction. To force the protein to adopt the required conformation, we constrained the distance between the catalytic hydrogen atom of Asp25B and the carbonyl oxygen atom of the substrate with an harmonic potential having an equilibrium length of 1.8 Å and a force constant of 50 kcal·mol^{-1}·Å^{-2}. The free energy cost of restraining the sampling to this subspace has been calculated before to be 4.6 kcal·mol^{-1}.[46] This contribution was added to all barriers. We ran another 5 ns MD with this new Hamiltonian. From the last structure of this 5 ns MD, three more simulations were launched with different seeds for the initial velocities, in order to provide sampling space for the subsequent work. Two of these simulations ran for 24 ns, and the other for 32 ns, to a total of 80 ns. The catalytic water is known to occupy the active site only transiently. Our MD simulations confirmed this experimental observation, as the catalytic water diffused away from the active site after a few tenths of nanoseconds. Any time that the catalytic water diffused from the active site, we stopped the simulations and started new simulations with the catalytic water inside the active site again. That is why we made three simulations, two with 24 ns and a third with 32 ns. These were the times during which the catalytic water remained in the active site.

Forty QM/MM models of the enzyme substrate complex were defined from 40 structures of the sampling dynamics equally spaced in time (i.e., with time intervals of 2 ns). For the ONIOM models, all water molecules were removed, except for the catalytic and structural ones. There were no water molecules on the inside of the protein except for these two. The solvent was removed from the calculations deliberately, and PCM calculations with a set of dielectric constants probed the effect of the environment (see below). Protease binds and cleaves two very large substrate polyproteins (Gag and Gag-Pol), much larger that protease itself (Gag-Pol has about 1500 residues). Most of the protease becomes buried in the substrate protein. Despite the enormous scientific and pharmacologic relevance of this complex, it has remained elusive to crystallography so far. It is unknown how much of protease is exposed to solvent and how much is buried in the binding partner. Additionally, protease acts after viral assembly, in a densely packed environment. To estimate the possible magnitude of environment effects, we performed single point energy calculations with an implicit solvation model (ONIOM-PCM), using different values for the dielectric constant (4, 10 and 80). As expected, higher dielectric constants lead to more pronounced changes in the calculated activation barrier, but the differences (in average 0.64 ± 0.57 kcal·mol^{-1} with ε = 4, 0.78 ± 0.72 kcal·mol^{-1} with ε = 10, and 0.81 ± 1.08 kcal·mol^{-1} with ε = 80) are not significant when compared to the range of activation barriers that is under study. Because the changes in activation barriers induced by solvation are negligible, and the real environment is not really known in detail, we report values corresponding to the enzyme without solvent. The effect of the environment in all calculated barriers is reported in the Supporting Information (Table S1 and Figure S1).

The reaction path was studied in the same manner for all models. We started by optimizing the reactants structure and subsequently scanning the reaction coordinate (i.e., the distance between the oxygen of the water nucleophile and the carbon of the peptide bond). The structure with the highest energy in the scan was identified and used as a guess to freely optimize the transition state. A frequency calculation was done to confirm the nature of the optimized structure. To obtain a reactant's structure in the same relative minimum as the transition state, we performed an IRC (intrinsic reaction coordinate) calculation in the reactant's direction for 10 steps. Instead of prolonging the IRC calculation all the way to the reactants, the last structure from the IRC was taken and freely optimized, while making sure that no structural rearrangements (independent from the reaction coordinate) occurred in this last optimization.

The different active site conformations were first analyzed with the aim of finding structural features correlated with the size of the barriers.[20] Here, we limited our analysis to bidimensional linear regression models, and used four interatomic distances as descriptors: (1) the hydrogen bond between Asp25A and the catalytic water, (2) the distance between the oxygen of the catalytic water and the carbonyl carbon in the peptide bond, (3) the hydrogen bond between the protonated Asp25B and the catalytic water, and (4) the hydrogen bond between Asp25B and the oxygen in the carbonyl group. Details about the performance of all regression models are provided in the Supporting Information.

In a second part of the analysis of the results, we employed a procedure to assess the influence of each MM layer residue in the activation energy of the reaction. For each of the optimized structures of reactants and transition states we did a series of single point energy calculations where we removed every single protein residue, substrate residue or structural water (a second water molecule is known to be present in the protease active center, which has only a structural role). This gives a total of 201 calculations for each pair (reactant and transition state) of optimized structures (196 protein residues, 4 substrate residues and the water molecule, all part of the low layer), or 402 calculations for each barrier; because we end up with 39 productive structures, we did more than 15 000 single point energy calculations in total. The influence of each residue in the barrier is given by the difference between the native barrier and the barrier calculated without the residue. A positive number means that the deleted residue increases the barrier, whereas a negative number means that the deleted residue decreases the barrier (it stabilizes the transition state more than it stabilizes the reactants). Note that the purpose of this procedure is to calculate the potential energy effect of each residue on the activation energy of the wild type enzyme. It is a conceptual quantity that cannot be measured experimentally. We are not trying to calculate the free activation energy of mutated enzymes, which is a different physical quantity. Our purpose is to understand if residues stabilize or destabilize the barrier at the specific transition state (TS) conformation, in absolute terms.

To measure reference distances between residues and the active site, we considered the following geometric points: the oxygen atom for the nucleophilic water; the amide carbonyl carbon for the substrate; the average atomic positions for

DOI: 10.1021/acscatal.5b00759
ACS Catal. 2015, 5, 5617−5626

neutral residues; the guanidine carbon for arginine residues; the nitrogen side chain for lysine residues; and the carboxylate carbon for aspartate and glutamate residues.

2.1. Molecular Dynamics Simulations Details. A total of 9960 water molecules were added to the protein in a rectangular box of 88 Å × 67 Å × 71 Å. At least 12 Å were left between the surface of the protein and the face of the box. Explicit van der Waals interactions were truncated at 10 Å, and the Coulombic interactions were calculated with the particle mesh Ewald (PME) method, with the real part also truncated at 10 Å.[49] A time step of 1 fs was used in simulations where the distance between the side chain proton of Asp25B, and the oxygen of the peptide bond was constrained with a harmonic potential. For simulations without this restriction, we used the SHAKE algorithm[50] and a time step of 2 fs. An initial warm-up dynamics of 100 ps (from 0 to 300 K) was done in the canonical ensemble (NVT). The production dynamics ran in the isothermal−isobaric ensemble (NPT) with the Langevin thermostat and isotropic position scaling, at 300 K and 1 bar. Parameters from the AMBER03 force field[51] were used for all the amino acids in the system, including the protein and peptide substrate. TIP3P water molecules[52] were used for the catalytic, structural, and solvent water molecules. Molecular mechanics simulations were done with the AMBER10 software.[53]

2.2. ONIOM Model Details. For the QM/MM calculations we divided the system into two layers. The high layer comprises the side chain of the two catalytic Aspartate residues, Asp25A and Asp25B, the water nucleophile, and 12 atoms of the substrate, as seen in Scheme 1. We deliberately used a very small QM layer in this study, for two reasons. The first is that the division represents the conceptual division between the "reacting atoms" and the "environment". It is much simpler and theoretically clear to define the "environment" at the MM level because MM allows us to clearly isolate the contributions of each atom or residue to the barrier. Second, as we are studying the reaction dozens of times, with transition state optimizations and IRC calculations (and more than 15 000 single point energy calculations), the use of a large QM layer would limit the number of conformations we could explore, which is the focus of the study. Besides, the choice of studying HIV-1 protease was made purposefully on this basis; it is a small protein, with only two catalytic residues and with a very well-known and undisputed catalytic mechanism. A larger QM layer would increase the accuracy of the energies but would not change them meaningfully. The MM layer includes all the remaining protein and substrate atoms, as well as the structural water molecule. The interaction between the layers was treated with the electrostatic embedding scheme. Comparable models have been used in the past to study the reaction mechanism of HIV-1 protease and similar enzymes.[38−41] The QM layer was optimized with the B3LYP[54,55] density functional and the 6-31G(d) basis-set,[56] while the MM layer was treated with the parm96 force field,[57] as implemented in the GAUSSIAN09 program. Sautet and co-workers have shown that B3LYP properly reproduces the geometries and energies of the first transition state of the HIV-1 protease reaction given by MP2 and CCSD(T).[39] The difference in activation energy between B3LYP/6-311++G(2d,2p) and CCSD(T)/6-311++G(d,p) levels of theory is only −0.6 kcal·mol^{-1}. The effect of the (D3) dispersion correction[58] was also calculated. Its contribution to the barrier was quite small (−1.0 kcal·mol^{-1} in average). Given the magnitude of the correction and the fact that B3LYP was shown to be excellent in reproducing the barrier for this transition state, we have not included the D3 correction in the results. The dispersion correction for every barrier is shown in the SI (Table S1 and Figure S2).

Zero point energies and entropic corrections were also calculated, in order to obtain free energies of activation. The 39 barriers of the native enzyme were recalculated with the 6-311+g(2d,2p) basis set. All ONIOM[59] calculations were done with GAUSSIAN09.[60]

Scheme 1. Different Mechanisms and Configurations Adopted by the Active Center of Protease[a]

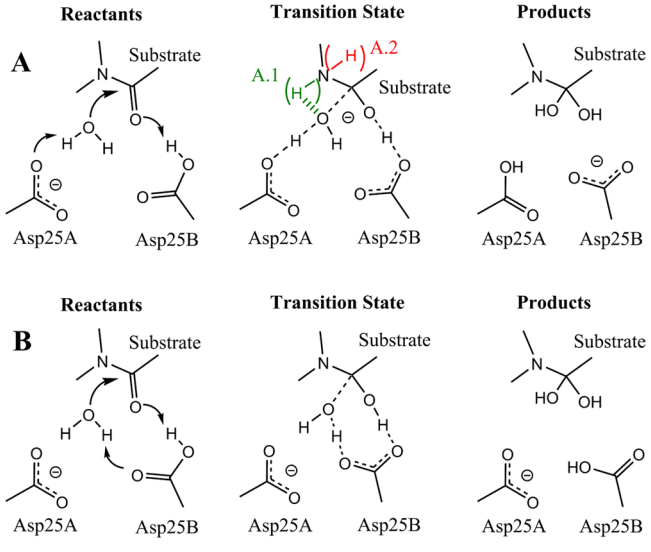

[a]Part A: The water nucleophile attacks the peptide bond and gives a proton to Asp25A. Depending on the configuration of the peptide bond when it loses the planarity, the nucleophile can be more or less stabilized by the highlighted hydrogen (configurations A.1 and A.2). This mechanism is the most commonly described in the literature. Part B: The water nucleophile attacks the peptide bond, but this time it gives its proton to Asp25B. In this unfavorable reaction path, Asp25A loses its catalytic role.

3. RESULTS

3.1. Fluctuations of the Free Activation Energies. Among the 40 initial reactant structures studied, only one was nonproductive. In this case, the optimization of the reactants led to a structure where Asp25B is making a hydrogen bond with Asp25A, instead of making it with the substrate. For the remaining 39 initial structures, we calculated the activation energies for the first step of the catalytic reaction of HIV-1 protease. We divided the barriers into three categories (A.1, A.2, and B) based on three clearly different conformations adopted by the active center. The first two categories (A.1 and A.2) are essentially the same mechanism, while B is a completely different path. Scheme 1 depicts these different paths, which are described later, and Table 1 summarizes their kinetic data. For variant A.1 of mechanism A, the average of the barriers is 27.5 kcal·mol^{-1} with a standard deviation (SD) of 6.6 kcal·mol^{-1}. The apparent barrier (i.e., the barrier that would be observed experimentally from a macroscopic population of enzymes in these initial states and proportion) was calculated using the transition state theory from the average of the k_{cat} values. Its value amounts to 16.2 kcal·mol^{-1}. For the variant A.2 of mechanism A, the average of the barriers is 31.9 kcal·mol^{-1}

DOI: 10.1021/acscatal.5b00759
ACS Catal. 2015, 5, 5617−5626

Table 1. Free Energies of Activation (kcal·mol^{-1}) and Rate Constant (s^{-1}) for the Three Mechanisms Found and Experimental Data[a]

mechanism	barrier range	average barrier	apparent barrier	K_{cat}
A.1	14.5−38.2	27.5 ± 6.6	16.2	24
A.2	23.2−41.1	31.9 ± 5.5	24.7	2.3×10^{-5}
B	38.5; 51.3	44.9 ± 9	38.9	2.3×10^{-15}
total	14.5−51.3	29.6 ± 7.5	16.5	15
experimental[61]			15.9	41 ± 6

[a]A correction of 4.6 kcal·mol^{-1} relative to the MD constraint is included in all the values.[46]

with and an SD of 5.5 kcal.mol^{-1}. The apparent barrier for this mechanism is 24.7 kcal·mol^{-1}. There are only 2 structures that followed mechanism B, one with a barrier of 38.5 kcal·mol^{-1}, the other with a barrier of 51.3 kcal·mol^{-1}. The average of these two barriers is 44.9 kcal·mol^{-1}, and the apparent barrier is 38.9 kcal·mol^{-1}. The overall barrier average for all structures is 29.6 kcal·mol^{-1}, with a standard deviation of 7.5, and the overall apparent barrier is 16.5 kcal·mol^{-1}. The experimental value for the overall free energy barrier of HIV-1 protease with this substrate, 15.9 kcal·mol^{-1},[61] which constitutes an upper limit for the chemical step, is in agreement with the overall apparent barrier.

The results shown here, and previously seen in other simulations as well,[18,23−26] indicate that the activation barriers of enzymes fluctuate significantly, and are often related to structural flexibility. We call these fluctuations *instantaneous disorder*. Protease, in less than 100 ns, presents many states with very different activation barriers. The observed (or apparent) k_{cat} is given by eq 1, where P_i is the probability of finding the enzyme in the reactant state i, and $\Delta G_i^{0‡}$ is the corresponding barrier free energy.

$$k_{cat} = k\frac{k_B T}{h}\sum_{i=1}^{n} P_i e^{-\Delta G_i^{0‡}/RT} \quad (1)$$

For the purpose of this work, we assumed that all reactants have equivalent probabilities. The probability of each barrier is accounted indirectly by the number of times the barrier appears in our 40 structures. Note that averaging the k_{cat} in this manner is not the same as averaging the activation energies and calculating k_{cat} from the average barrier. The k_{cat} calculated from the average of the barriers has no physical meaning, and cannot be associated with any experimental value.

The general model that explains these results is depicted in Figure 1. The enzyme goes through many conformations, which are associated with different barriers (instantaneous disorder). Independently, the energy accumulated on the reaction coordinate also fluctuates. The reaction occurs when the energy localized on the reaction coordinate is higher than the current instantaneous barrier. The height of this barrier is essentially determined by the structure of the enzyme as it is in the reactants state, because the enzyme has no time to go through large rearrangements within the time scale of a molecular vibration: the time the chemical reaction takes to occur.

The observation of these large fluctuations in the catalytic barriers is not new. In the case of protease, a decrease in the activation barrier from ∼50 kcal·mol^{-1} to ∼20 kcal·mol^{-1} was previously reported, as the substrate approximates the catalytic aspartates.[62] We obtain a similar effect when we compare mechanism B to mechanism A. Additionally, HIV-1 protease is able to undergo relatively large structural rearrangements in the flaps region,[63] which also must affect catalysis. On a microsecond time scale, these flap movements are associated mostly with substrate entry and exit,[64−67] and are important to understand the full catalytic cycle of HIV protease, in particular because product exit is thought to be rate-limiting in physiological conditions. However, because in the present work we are mostly concerned with the motions that directly affect the catalytic step, we focused instead on conformational fluctuations occurring when the substrate is bound to the protease, and the flaps are in the closed state.

In other enzymes, such as ketosteroid isomerase, small changes in active site hydration (the entry of two additional water molecules around the catalytic Asp38), driven by a protein conformational change that closes/opens the active site, induced a raise in the free energy barrier of around 20 kcal/mol.[68] Variations up to 17 kcal·mol^{-1} were also observed in the P450 catalyzed epoxidation and hydroxylation of propene and cyclohexene.[69] In this case, the origin of the variation seems to stem from the multiple possible substrate orientations, a factor that is expected to be particularly relevant when promiscuous enzymes bind small substrates. In the case of fatty acid amide hydrolase, 36 different barriers were derived, with a free energy span of about 11 kcal/mol.[20] In that work, the authors carried out a successful statistical analysis that identified the specific residues/interactions that were responsible for most of the observed differences.

There has been a long-standing debate about the relationship between enzyme dynamics and enzyme catalysis.[70] We do not consider the fluctuations we observed here, "dynamic effects", in the sense that they are not dynamically coupled to movements along the reaction coordinate. We consider that the movement along the reaction coordinate is much faster than the movement along other orthogonal directions in the PES. The roughness of the time-dependent PES and the subsequent instantaneous barriers arise from a thermal equilibrium distribution. The conformations explored here are just specific substates of the whole macroscopic ensemble. Additionally, we rationalize their effect through the TST without any role of the transmission factor.

The effect of tunneling will be small compared to the fluctuations in activation free energy that are originated by the different enzyme conformations. However, this effect will be different from conformation to conformation, as the height and the width of the barriers changes, and will be more relevant for the lower barriers, that also contribute more to the observed activation free energy.

3.2. Effect of Conformational Fluctuations in Catalysis. After analyzing the 40 structures of reactants and transition states, we found three factors that account for the fluctuations, as follows:

1. Different Reaction Mechanisms (Scheme 1). Two structures follow a mechanism other than the path described in the literature for HIV-1 protease (path B). In this mechanism, Asp25A loses its role in the reaction, and the proton of the nucleophile goes to the free oxygen atom of Asp25B instead. Because the oxygen atom of Asp25B is less electronegative than the oxygen atom of Asp25A, the proton of the nucleophile is less stabilized in the transition state, which becomes more energetic.

2. Different Active Center Conformations. The hydrogen atom of the scissile amine bond is found in two conformations.

DOI: 10.1021/acscatal.5b00759
ACS Catal. 2015, 5, 5617−5626

In the A.1 position, the hydrogen is making a hydrogen bond with the attacking hydroxide. This interaction stabilizes the negative charge that builds up in the hydroxide in the TS. On the A.2 position, the hydroxide faces the lone electron pair of the amide nitrogen, a repulsive arrangement that leads to higher activation energies.

We also found that simple geometrical descriptors, such as key interatomic distances, correlate well with differences in the activation barriers.[20,62,68] We have chosen four obvious distances directly related to the reaction coordinate (definitions for these distances are provided in the Methods section). We built all possible regression models using up to two explanatory variables (distances). Figure 2 illustrates the performance of the best one-dimensional model and the best two-dimensional model, both providing satisfactory predictive power. The single variable displaying the highest correlation with the activation barrier is the distance corresponding to the hydrogen bond between the catalytic water and Asp25A "Asp−Wat". From the chemical viewpoint, this result is intimately associated with the reaction coordinate: it represents the importance of abstracting a proton from the water in order to allow the attack on the carbonyl group. The best bi-dimensional regression model added the "Wat−Pep" distance (the distance between the water oxygen and the carbonyl carbon) to the already discussed Asp−Wat, increasing R^2 from 0.53 to 0.69. This second distance completes the chemical path linking Asp25A and the carbonyl group in the peptide bond. It is worthy to note that the largest change in charge distribution along the reaction coordinate is precisely between Asp25A and the peptide bond (see Scheme 2).

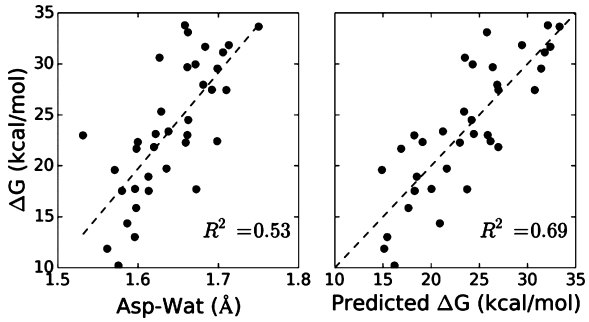

Figure 2. Correlation between activation barriers and key interatomic distances. The plot on the left side shows the computed activation barriers as a function of the shortest distance between a proton of the catalytic water and a carboxylic oxygen of Asp25A ("Asp−Wat" distance). On the right side, the *x*-axis represents the predicted activation barrier using linear regression with two explanatory variables: the "Asp−Wat" distance and the distance between the oxygen in the catalytic water and the carbonyl carbon in the peptide bond ("Wat−Pep" distance).

The results shown in Figure 2 indicate that simple bidimensional regressions are insufficient to explain quantitatively the wealth of different barriers that protease shows within a few nanoseconds. Instead of introducing more explanatory variables into the model, we looked for the physical sources of these fluctuations and analyzed the contribution of each individual residue to the energy barrier.

3. Conformational Fluctuations. Conformational fluctuations in the rest of the enzyme structure affect the barrier through electrostatic interactions. The sign and size of each residue contribution to the barrier (stabilization of destabilization) can be explained by looking at the flow of negative charge along the reaction path (see Scheme 2). The rest of the discussion will focus on this effect.

Scheme 2. Flow of Negative Charge That Occurs along the Reaction Coordinate

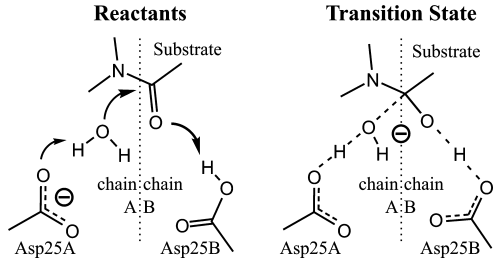

Before addressing the problem of the residues' contributions to the activation energy fluctuations, it will be instructive to focus first on explaining how the residues affect the catalytic barriers. The results we obtained in this respect are extremely intuitive and consistent. To begin with, it is fairly noticeable that residues near the active center have a greater influence on catalysis than the more distant ones (Figure 3).

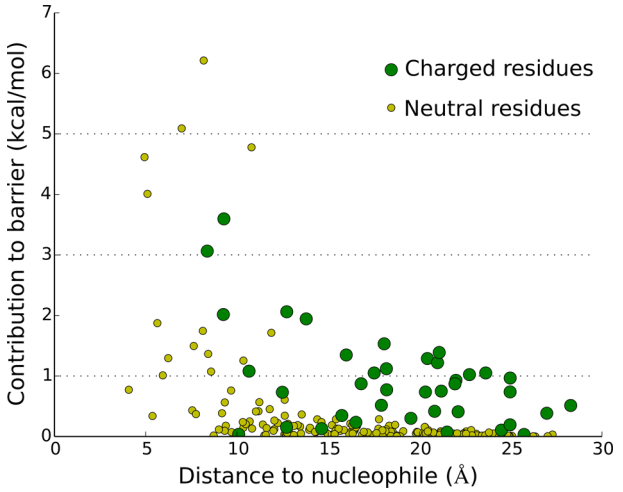

Figure 3. Averaged contribution of each residue for the reaction barrier (absolute values), plotted against the (average) distance of the residue to the nucleophilic water oxygen.

The decay is very fast to neutral residues, but less accentuated to charged ones. The effect of charged residues is still meaningful even at distances of 20 Å from the active center. As for neutral residues, after 10 Å, the influence is already negligible. As clearly shown, most of the contribution (either positive or negative) of neutral residues on the activation energy comes from the first layer of residues around the active center. The interpretation on charged residues is more complicated. Even if we admit that ignoring a 1 kcal·mol^{-1} contribution for a single residue at 20 Å of the active center is acceptable, ignoring dozens of such contributions is not prudent. All these residues are moving, and their charge is affecting the barrier, the dispersion in the values of individual barriers could be significant, even if these movements do not affect the average barrier. Because the apparent barrier is dominated by contributions of these transient smaller barriers, these fluctuations are of the upmost importance.

DOI: 10.1021/acscatal.5b00759
ACS Catal. 2015, 5, 5617−5626

The contribution of each residue toward stabilizing or destabilizing the TS is easy to rationalize if we explain it against the charge transfer that takes place when the system evolves from the reactants to the transition state. As seen on Scheme 2, in the reactants, the negative charge on the active center is localized on Asp25, whereas in the transition state, the charge is delocalized through the active center but centered on the substrate and hydroxide ion. The net transfer of negative charge is then upward and rightwards. It is expected that residues that help the rearrangement of electronic density toward the transition state configuration will lower the activation barrier and residues that stabilize negative charge in Asp25A will increase the barrier, which we have demonstrated. In other words, if we consider the orientation shown in Scheme 2, positive residues in the upper right corner stabilize the transition state, and in the lower left, they stabilize the reactants. The opposite is true for negative residues.

This interpretation is also extensive to neutral residues, if we consider their partial charges. If the positive partial charge is closer to the active center than the negative partial charge, the residue will behave as if it was a positive residue, and vice versa. The effect of neutral residues will decay faster than the effect of charged residues, because the partial charges are small and add to zero, with a counterbalancing charge almost at the same distance from the active center. The neutral residues that significantly affect the barrier and their average contribution to the activation energy are depicted in Figure 4. A negative

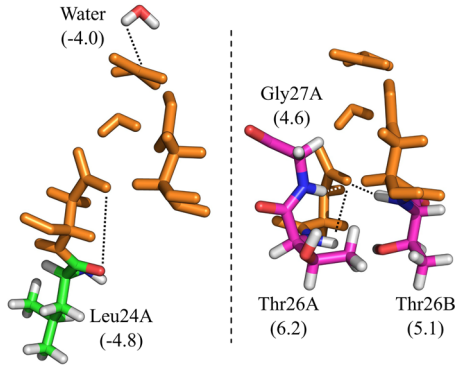

Figure 4. Neutral residues that have the most impact on the activation energies. Residues with a negative value of contribution lower the barrier, and are represented with green carbons at the left. Residues with a positive value of contribution increase the barrier and are represented with purple carbons at the right. The catalytic aspartates, the nucleophile and the substrate are colored in orange. Energies are in kcal·mol^{-1}.

number means that the residue lowers the activation energy, whereas a positive value means that the residue increases the activation energy. Leu24 and the structural water molecule are the residues that decrease the barrier to a greater extent. They do it by opposite effects: the structural water molecule stabilizes the transition state with a positive partial charge near the peptide bond. Instead, Leu24 destabilizes the reactants by having its carbonyl group near the side chain of Asp25. The other three residues increase the barrier in a similar (but opposite) way, by having the hydrogen atom of the peptide bond very close to Asp25A. Gly27A and Thr24B establish a hydrogen bond with the Asp25A carboxylate. These five residues are extremely close to the active center and have a very marked impact on the activation energies. To be more confident on the magnitude of these values, it would be desirable to use a model where these residues are included in the high layer of the ONIOM calculations, but there is no reason to think that such approach would change the conclusions in a meaningful way. Moreover, if we wanted to use a higher theoretical level we would have to decrease the sampling to compensate for the additional computational cost, and that trade does not seem to be advantageous in the context of this study.

We now extend the analysis to all residues (neutral and charged) that affect the barrier by more than 0.5 kcal·mol^{-1}. In Figure 5, these residues are represented in sticks, whereas the

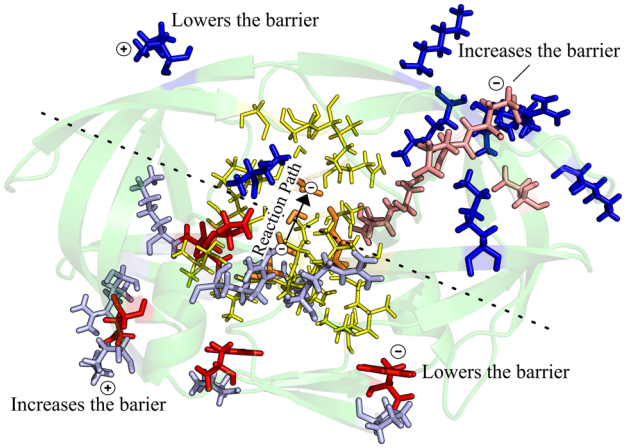

Figure 5. Representation of the protease enzyme with the residues that affect more the activation energy (>0.5 kcal·mol^{-1}). The catalytic aspartates, the nucleophile and the portion of the substrate in the high layer are colored in orange. Neutral residues are colored in yellow. Positively charged residues that decrease the activation energy are colored in dark blue, and positively charged residues that increase the barrier are colored in light blue. Negatively charged residues that decrease the activation energy are colored in red, and negatively charged residues that increase the barrier are colored in pink. The arrow represents the redistribution of negative charge from the reactants to the transition state.

rest of the protein is represented in ribbons. All the information on this figure is coherent with the interpretation we have been outlining. Neutral residues that affect the barrier significantly (in yellow) form a tight core around the active center (the contributions of all neutral residues are included in the SI). Positive residues that are closer to the peptide bond (dark blue) stabilize the barrier, while positive residues that are closer to Asp25A (light blue) increase the activation energy. For negative residues, the opposite holds: residues near Asp25A (in red) are those that decrease the activation energy, while residues that increase it are near the peptide bond (in pink).

In Figure 6, this same information is shown quantitatively. The contribution of the residues to the barrier is plotted against the difference between the distance of the residue to Asp25A and the distance of the residue to the peptide bond. Again, a positive energy value means that the residue increases the barrier by that amount, while a negative value means the residues stabilizes the barrier. Once more, the pattern is consistent with our previous results: positive residues populate the lower left and upper right quadrants; and negative residues populate the upper left and lower right quadrants. Furthermore, the greater the difference between the distances, the greater is the influence of the charged residues.

DOI: 10.1021/acscatal.5b00759
ACS Catal. 2015, 5, 5617−5626

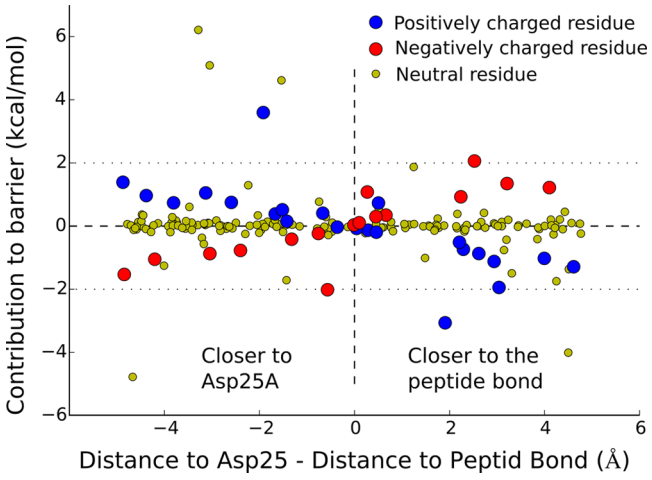

Figure 6. Averaged contribution to the barrier for each residue plotted against the difference of the distance between the residue and Asp25, and the distance between the residue and the peptide bond to be cleaved.

After establishing how and by how much the protein amino acids influence catalysis, we are ready to tackle the original question: Do fluctuations in the protein structure justify the dispersion observed in the catalytic barriers? Figure 7 is a plot

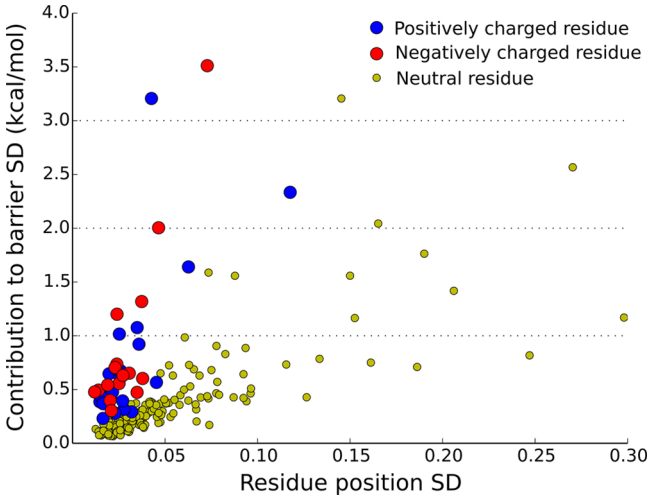

Figure 7. Standard deviation of the contribution of the residues to the barrier plotted against the standard deviation of the relative residue position. This last value is calculated as ((distance to Asp25A − distance to peptide bond)/average distance to active center).

of the standard deviation of the residues contribution to catalysis against the standard deviation of their distance to the active center. The figure tells us that certain residues move significantly from state to state, and that this movement affects the activation barrier significantly, especially if the residues are charged, or near the active center.

This result is more than enough to justify the dispersion of the activation energies. Considering that the contribution of each residue follows a normal distribution and the movement of the residues is not correlated, we can calculate the expected overall dispersion of results to be 10.2 kcal·mol^{-1}, by the quadratic sum of the individual SDs. This value is the maximum deviation obtainable for the case where there is no correlation among residues (note that large-scale correlated movements can make these fluctuations wider, not smaller. Such backbone fluctuations and their effects over the turnover have been discussed before.[71] However, at the time scale studied here they are not present). The actual value for the protease system is smaller, 6.6 kcal·mol^{-1} (for mechanism A.1), due to the existence of correlation between residues. Positive and negative residues interacting with their side chains, for example, will move in tandem, and will cancel each other in terms of contribution to the activation energy. This result gives us enough confidence to assert that enzyme structure fluctuations are responsible for the activation fluctuations.

4. CONCLUSIONS

In this study, we aimed at a better understanding of the effect of conformational fluctuations in the activation free energy of enzymatic reactions by using a computational model of HIV-1 Protease. We took 40 equally time spaced snapshots from 80 ns of MD simulations, and we used these structures as initial points for subsequent QM/MM studies of the reaction path first step. The results show that, along time, the enzyme goes through many reactant states that are associated with different activation energies (*instantaneous disorder*), from 14.5 kcal·mol^{-1} up to 51.3 kcal·mol^{-1}. The results point to a disordered energetic landscape where the barrier associated with each microstate varies several orders of magnitude in very short periods of time (ns). The overall apparent barrier calculated from 39 productive structures is 16.5 kcal·mol^{-1}, which is in very good agreement with the experimental barrier of 15.9 kcal·mol^{-1} for product release.

In the second part of the work, we tried to understand the reasons behind such diversity in the activation energies of different microstates. We identified three main causes. The first is the existence of a different mechanism, where the role of Asp25A is diminished. The second is related to different conformation of the active center, in particular, the orientation of a single proton and two key distances along the reaction path. The proton in question is bonded to the nitrogen atom of the peptide bond to be broken. In the main conformation, it is orientated toward the nucleophile and helps in the stabilization of the transition state. On the other conformation, it is pointing to the opposite side. With respect to the two interatomic distances associated with the reaction coordinate, we found that when the distances at the reactants are closer to the transition state conformation, the associated barriers are smaller. The third reason for the large span in the activation barriers is explained by variations in the electrostatic environment of the active site, due to distinct structural conformations of the rest of the enzyme. The contribution of the residues to the instantaneous barrier is related to their influence on the movement of electronic charge from the reactants to the transition state. A negative charge near Asp25A, for example, pushes the negative charge away from Asp25A, destabilizing the reactants state and stabilizing the transition state. The contribution of each residue also fluctuates along time, according to its position relative to the active center. The fluctuations of all residues taken together are enough to justify the overall dispersion observed in the activation energies.

We think our results are of significance to a better understanding of enzymatic catalysis in general. We show very clearly that the conformational and catalytic landscape of enzymes is very heterogeneous and that this heterogeneity can be traced back not only to different active site conformations but also to fluctuating interatomic interactions with the rest of

DOI: 10.1021/acscatal.5b00759
ACS Catal. 2015, 5, 5617−5626

the enzyme. Most importantly, we have shown that the fluctuations in the barriers are fundamental for the enzymatic rate constant, as most of the products will be formed by a very few transient enzyme conformations that provide very low barriers.

■ ASSOCIATED CONTENT

Supporting Information

The Supporting Information is available free of charge on the ACS Publications website at DOI: 10.1021/acscatal.5b00759.

Energies of all native reactants and transition state structures (TXT)

Energies of all truncated reactants and transition state structures (TXT)

Structures of all conformations in the reactants and transition state (ZIP)

Table with contributions from zero point energy, thermal and entropic corrections to the enzyme/substrate system, solvation free energy and dispersion correction (D3). Figure with the effect of enzyme solvation on calculated activation barriers. Figure with the contribution of D3 dispersion corrections to activation barriers. Figure with the linear regression models based on interatomic distances (PDF)

■ AUTHOR INFORMATION

Corresponding Author

*E-mail: pafernan@fc.up.pt.

Notes

The authors declare no competing financial interest.

■ ACKNOWLEDGMENTS

This work has been funded by FEDER/COMPETE and Fundação para a Ciência e a Tecnologia (FCT) through grants PEst-C/EQB/LA0006/2011 and EXCL/QEQ-COM/0394/2012. A.J.M.R. thanks FCT for a postdoctoral scholarship (SFRH/BPD/94883/2013). D.S.M. thanks FCT for a doctoral scholarship SFRH/BD/84922/2012.

■ REFERENCES

(1) Kohen, A. *Acc. Chem. Res.* **2015**, *48* (2), 466−473.

(2) Callender, R.; Dyer, R. B. *Acc. Chem. Res.* **2015**, *48* (2), 407−413.

(3) Henzler-Wildman, K.; Kern, D. *Nature* **2007**, *450*, 964−972.

(4) Boehr, D. D.; McElheny, D.; Dyson, H. J.; Wright, P. E. *Science* **2006**, *313* (5793), 1638−1642.

(5) Smiley, R. D.; Hammes, G. G. *Chem. Rev.* **2006**, *106* (8), 3080−3094.

(6) Lu, H. P.; Xun, L.; Xie, X. S. *Science* **1998**, *282* (5395), 1877−1882.

(7) Xue, Q.; Yeung, E. S. *Nature* **1995**, *373* (6516), 681−683.

(8) English, B. P.; Min, W.; van Oijen, A. M.; Lee, K. T.; Luo, G.; Sun, H.; Cherayil, B. J.; Kou, S. C.; Xie, X. S. *Nat. Chem. Biol.* **2006**, *2* (2), 87−94.

(9) Craig, D. B.; Arriaga, E. A.; Wong, J. C. Y.; Lu, H.; Dovichi, N. J. *J. Am. Chem. Soc.* **1996**, *118* (22), 5245−5253.

(10) Shi, J.; Palfey, B. A.; Dertouzos, J.; Jensen, K. F.; Gafni, A.; Steel, D. *J. Am. Chem. Soc.* **2004**, *126* (22), 6914−6922.

(11) Ha, T.; Ting, A. Y.; Liang, J.; Caldwell, W. B.; Deniz, A. A.; Chemla, D. S.; Schultz, P. G.; Weiss, S. *Proc. Natl. Acad. Sci. U. S. A.* **1999**, *96* (3), 893−898.

(12) Terentyeva, T. G.; Engelkamp, H.; Rowan, A. E.; Komatsuzaki, T.; Hofkens, J.; Li, C. B.; Blank, K. *ACS Nano* **2012**, *6* (1), 346−354.

(13) Friesner, R. A.; Guallar, V. *Annu. Rev. Phys. Chem.* **2005**, *56*, 389−427.

(14) Senn, H.; Thiel, W. QM/MM Methods for Biological Systems. In *Atomistic Approaches in Modern Biology*; Reiher, M., Ed.; Springer: Berlin, Heidelberg, 2007; Vol. *268*, pp 173−290.

(15) Mulholland, A. J. *J. R. Soc., Interface* **2008**, *5* (Suppl 3), 169−172.

(16) Senn, H. M.; Thiel, W. *Angew. Chem., Int. Ed.* **2009**, *48* (7), 1198−1229.

(17) Sousa, S. F.; Fernandes, P. A.; Ramos, M. J. *Phys. Chem. Chem. Phys.* **2012**, *14* (36), 12431−12441.

(18) Ferrer, S.; Tuñón, I.; Martí, S.; Moliner, V.; Garcia-Viloca, M.; González-Lafont, À.; Lluch, J. M. *J. Am. Chem. Soc.* **2006**, *128* (51), 16851−16863.

(19) Sanchez-Martinez, M.; Marcos, E.; Tauler, R.; Field, M.; Crehuet, R. *J. Phys. Chem. B* **2013**, *117*, 14261−14272.

(20) Lodola, A.; Sirirak, J.; Fey, N.; Rivara, S.; Mor, M.; Mulholland, A. J. *J. Chem. Theory Comput.* **2010**, *6*, 2948−2960.

(21) Roca, M.; Messer, B.; Hilvert, D.; Warshel, A. *Proc. Natl. Acad. Sci. U. S. A.* **2008**, *105*, 13877−13882.

(22) Benkovic, S. J.; Hammes, G. G.; Hammes-Schiffer, S. *Biochemistry* **2008**, *47*, 3317−3321.

(23) Hu, P.; Zhang, Y. *J. Am. Chem. Soc.* **2006**, *128* (4), 1272−1278.

(24) Lodola, A.; Mor, M.; Zurek, J.; Tarzia, G.; Piomelli, D.; Harvey, J. N.; Mulholland, A. J. *Biophys. J.* **2007**, *92* (2), L20−L22.

(25) Ribeiro, A. J.; Ramos, M. J.; Fernandes, P. A. *J. Am. Chem. Soc.* **2012**, *134* (32), 13436−13447.

(26) Zhang, Y.; Kua, J.; McCammon, J. A. *J. Phys. Chem. B* **2003**, *107* (18), 4459−4463.

(27) Fitzgerald, P. M.; Springer, J. P. *Annu. Rev. Biophys. Biophys. Chem.* **1991**, *20*, 299−320.

(28) Louis, J. M.; Ishima, R.; Torchia, D. A.; Weber, I. T. HIV-1 Protease: Structure, Dynamics, and Inhibition. In *Advances in Pharmacology*; Kuan-Teh, J., Ed.; Elsevier: Amsterdam, 2007; Vol. *55*, pp 261−298.

(29) Hyland, L. J.; Tomaszek, T. A.; Meek, T. D. *Biochemistry* **1991**, *30* (34), 8454−8463.

(30) Miller, M.; Schneider, J.; Sathyanarayana, B.; Toth, M.; Marshall, G.; Clawson, L.; Selk, L.; Kent, S.; Wlodawer, A. *Science* **1989**, *246* (4934), 1149−1152.

(31) Northrop, D. B. *Acc. Chem. Res.* **2001**, *34* (10), 790−797.

(32) Polgar, L.; Szeltner, Z.; Boros, I. *Biochemistry* **1994**, *33* (31), 9351−9357.

(33) Prabu-Jeyabalan, M.; Nalivaika, E.; Schiffer, C. A. *J. Mol. Biol.* **2000**, *301* (5), 1207−1220.

(34) Rodriguez, E. J.; Angeles, T. S.; Meek, T. D. *Biochemistry* **1993**, *32* (46), 12380−12385.

(35) Suguna, K.; Padlan, E. A.; Smith, C. W.; Carlson, W. D.; Davies, D. R. *Proc. Natl. Acad. Sci. U. S. A.* **1987**, *84* (20), 7009−7013.

(36) Das, A.; Mahale, S.; Prashar, V.; Bihani, S.; Ferrer, J. L.; Hosur, M. V. *J. Am. Chem. Soc.* **2010**, *132* (18), 6366−6373.

(37) Kovalevsky, A. Y.; Chumanevich, A. A.; Liu, F.; Louis, J. M.; Weber, I. T. *Biochemistry* **2007**, *46* (51), 14854−14864.

(38) Piana, S.; Bucher, D.; Carloni, P.; Rothlisberger, U. *J. Phys. Chem. B* **2004**, *108* (30), 11139−11149.

(39) Garrec, J.; Sautet, P.; Fleurat-Lessard, P. *J. Phys. Chem. B* **2011**, *115* (26), 8545−8558.

(40) Carnevale, V.; Raugei, S.; Piana, S.; Carloni, P. *Comput. Phys. Commun.* **2008**, *179* (1−3), 120−123.

(41) Bras, N. F.; Ramos, M. J.; Fernandes, P. A. *Phys. Chem. Chem. Phys.* **2012**, *14* (36), 12605−12613.

(42) Bora, R. P.; Barman, A.; Zhu, X.; Ozbil, M.; Prabhakar, R. *J. Phys. Chem. B* **2010**, *114* (33), 10860−10875.

(43) Beveridge, A. J. *J. Mol. Struct.: THEOCHEM* **2009**, *900* (1−3), 1−8.

(44) Singh, R.; Barman, A.; Prabhakar, R. *J. Phys. Chem. B* **2009**, *113* (10), 2990−2999.

(45) Bjelic, S.; Åqvist, J. *Biochemistry* **2006**, *45* (25), 7709−7723.

(46) Sadiq, S. K.; Coveney, P. V. *J. Chem. Theory Comput.* **2014**, *11* (1), 316−324.

DOI: 10.1021/acscatal.5b00759
ACS Catal. 2015, 5, 5617−5626

(47) Miller, M.; Schneider, J.; Sathyanarayana, B. K.; Toth, M. V.; Marshall, G. R.; Clawson, L.; Selk, L.; Kent, S. B. H.; Wlodawer, A. *Science* **1989**, *246* (4934), 1149−1152.
(48) Dennington II, R.; Keith, T.; Millam, J. *GaussView*, Version 5; Semichem Inc.: Shawnee Mission, KS, 2009.
(49) Essmann, U.; Perera, L.; Berkowitz, M. L.; Darden, T.; Lee, H.; Pedersen, L. G. *J. Chem. Phys.* **1995**, *103* (19), 8577−8593.
(50) Ryckaert, J. P.; Ciccotti, G.; Berendsen, H. J. C. *J. Comput. Phys.* **1977**, *23* (3), 327−341.
(51) Ponder, J. W.; Case, D. A. Force Fields for Protein Simulations. In *Advances in Protein Chemistry*; Valerie, D., Ed. Elsevier: Amsterdam, 2003; Vol. *66*, pp 27−85.
(52) Jorgensen, W. L.; Chandrasekhar, J.; Madura, J. D.; Impey, R. W.; Klein, M. L. *J. Chem. Phys.* **1983**, *79* (2), 926−935.
(53) Case, D. A.; Darden, T. A.; Cheatham; Simmerling, C. L.; Wang, J.; Duke, R. E.; Luo, R.; Crowley, M.; Walker, R. C.; Zhang, W.; Merz, K. M.; Wang, B.; Hayik, S.; Roitberg, A.; Seabra, G.; Kolossváry, I.; Wong, K. F.; Paesani, F.; Vanicek, J.; Wu, X.; Brozell, S. R.; Steinbrecher, T.; Gohlke, H.; Yang, L.; Tan, C.; Mongan, J.; Hornak, V.; Cui, G.; Mathews, D. H.; Seetin, M. G.; Sagui, C.; Babin, V.; Kollman, P. A. *AMBER 10*; University of California: San Francisco, 2008.
(54) Becke, A. D. *J. Chem. Phys.* **1993**, *98*, 5648.
(55) Lee, C.; Yang, W.; Parr, R. G. *Phys. Rev. B: Condens. Matter Mater. Phys.* **1988**, *37*, 785−789.
(56) Ditchfield, R.; Hehre, W. J.; Pople, J. A. *J. Chem. Phys.* **1971**, *54*, 724.
(57) Cornell, W. D.; Cieplak, P.; Bayly, C. I.; Gould, I. R.; Merz, K. M.; Ferguson, D. M.; Spellmeyer, D. C.; Fox, T.; Caldwell, J. W.; Kollman, P. A. *J. Am. Chem. Soc.* **1995**, *117* (19), 5179−5197.
(58) Grimme, S.; Antony, J.; Ehrlich, S.; Krieg, H. *J. Chem. Phys.* **2010**, *132* (15), 154104.
(59) Vreven, T.; Byun, K. S.; Komaromi, I.; Dapprich, S.; Montgomery, J. A.; Morokuma, K.; Frisch, M. J. *J. Chem. Theory Comput.* **2006**, *2* (3), 815−826.
(60) Frisch, M. J.; Trucks, G. W.; Schlegel, H. B.; Scuseria, G. E.; Robb, M. A.; Cheeseman, J. R.; Scalmani, G.; Barone, V.; Mennucci, B.; Petersson, G. A.; Nakatsuji, H.; Caricato, M.; Li, X.; Hratchian, H. P.; Izmaylov, A. F.; Bloino, J.; Zheng, G.; Sonnenberg, J. L.; Hada, M.; Ehara, M.; Toyota, K.; Fukuda, R.; Hasegawa, J.; Ishida, M.; Nakajima, T.; Honda, Y.; Kitao, O.; Nakai, H.; Vreven, T.; Montgomery Jr, J. A.; Peralta, J. E.; Ogliaro, F.; Bearpark, M.; Heyd, J. J.; Brothers, E.; Kudin, K. N.; Staroverov, V. N.; Kobayashi, R.; Normand, J.; Raghavachari, K.; Rendell, A.; Burant, J. C.; Iyengar, S. S.; Tomasi, J.; Cossi, M.; Rega, N.; Klene, M.; Knox, J. E.; Cross, J. B.; Bakken, V.; Adamo, C.; Jaramillo, J.; Gomperts, R.; Stratmann, R. E.; Yazyev, O.; Austin, A. J.; Cammi, R.; Pomelli, C.; Ochterski, J. W.; Martin, R. L.; Morokuma, K.; Zakrzewski, V. G.; Voth, G. A.; Salvador, P.; Dannenberg, J. J.; Dapprich, S.; Daniels, A. D.; Farkas, Ö.; Foresman, J. B.; Ortiz, J. V.; Cioslowski, J.; Fox, D. J. *Gaussian 09*, Revision A.02; Gaussian, Inc.: Wallingford, CT, 2009.
(61) Maschera, B.; Darby, G.; Palú, G.; Wright, L. L.; Tisdale, M.; Myers, R.; Blair, E. D.; Furfine, E. S. *J. Biol. Chem.* **1996**, *271* (52), 33231−33235.
(62) Piana, S.; Carloni, P.; Parrinello, M. *J. Mol. Biol.* **2002**, *319* (2), 567−583.
(63) Perryman, A. L.; Lin, J. H.; McCammon, J. A. *Protein Sci.* **2004**, *13* (4), 1108−1123.
(64) Chang, C. E.; Trylska, J.; Tozzini, V.; McCammon, J. A. *Chem. Biol. Drug Des.* **2007**, *69* (1), 5−13.
(65) Tozzini, V.; Trylska, J.; Chang, C. E.; McCammon, J. A. *J. Struct. Biol.* **2007**, *157* (3), 606−615.
(66) Trylska, J.; Tozzini, V.; Chang, C. A.; McCammon, J. A. *Biophys. J.* **2007**, *92* (12), 4179−4187.
(67) Hamelberg, D.; McCammon, J. A. *J. Am. Chem. Soc.* **2005**, *127* (40), 13778−13779.
(68) van der Kamp, M. W.; Chaudret, R.; Mulholland, A. J. *FEBS J.* **2013**, *280* (13), 3120−3131.
(69) Lonsdale, R.; Harvey, J. N.; Mulholland, A. J. *J. Phys. Chem. B* **2010**, *114* (2), 1156−1162.
(70) Kamerlin, S. C. L.; Warshel, A. *Proteins: Struct., Funct., Genet.* **2010**, *78* (6), 1339−1375.
(71) Carnevale, V.; Raugei, S.; Micheletti, C.; Carloni, P. *J. Am. Chem. Soc.* **2006**, *128* (30), 9766−9772.

DOI: 10.1021/acscatal.5b00759
ACS Catal. 2015, 5, 5617−5626